symmetry

MDPI

Article

Statistical Inference and Application of Asymmetrical Generalized Pareto Distribution Based on Peaks-Over-Threshold Model

Wenru Chen [1], Xu Zhao [1,*,†], Mi Zhou [2,*], Haiqing Chen [3], Qingqing Ji [4,5] and Weihu Cheng [1]

[1] School of Mathematics, Statistics and Mechanics, Beijing University of Technology, Beijing 100124, China; chenwenru@emails.bjut.edu.cn (W.C.); chengweihu@bjut.edu.cn (W.C.)
[2] China National Environmental Monitoring Center, Beijing 100012, China
[3] School of Economics, Nanjing University of Finance and Economics, Nanjing 210023, China; 9120181077@nufe.edu.cn
[4] University of Chinese Academy of Sciences, Beijing 100049, China; jiqingqing20b@ict.ac.cn
[5] Institute of Computing Technology, Chinese Academy of Sciences, Beijing 100190, China
* Correspondence: zhaox@bjut.edu.cn (X.Z.); zhoumi@cnemc.cn (M.Z.)
† Current address: No.100, Pingleyuan, Chaoyang District, Beijing 100124, China.

Abstract: Generalized Pareto distribution (GPD), an asymmetrical distribution, primarily models exceedances over a high threshold in many applications. Within the peaks-over-threshold (POT) framework, we consider a new GPD parameter estimation method to estimate a common tail risk measure, the value at risk (VaR). The proposed method is more suitable for the POT framework and makes full use of data information. Specifically, our estimation method builds upon the generalized probability weighted moments method and integrates it with the nonlinear weighted least squares method. We use exceedances for the GPD, minimizing the sum of squared differences between the sample and population moments of a function of GPD random variables. At the same time, the proposed estimator uses three iterations and assigns weight to further improving the estimated performance. Under Monte Carlo simulations and with a real heavy-tailed dataset, the simulation results show the advantage of the newly proposed estimator, particularly when VaRs are at high confidence levels. In addition, by simulating other heavy-tailed distributions, our method still exhibits good performance in estimating misjudgment distributions.

Keywords: generalized Pareto distribution; parameter estimation; extreme quantile estimation; extreme value theory

Citation: Chen, W.; Zhao, X.; Zhou, M.; Chen, H.; Ji, Q.; Cheng, W. Statistical Inference and Application of Asymmetrical Generalized Pareto Distribution Based on Peaks-Over-Threshold Model. *Symmetry* **2024**, *16*, 365. https://doi.org/10.3390/sym16030365

Academic Editors: Arne Johannssen, Nataliya Chukhrova and Quanxin Zhu

Received: 6 February 2024
Revised: 1 March 2024
Accepted: 8 March 2024
Published: 18 March 2024

1. Introduction

Some scholars have found that the tails of various measured data distributions tend to be heavier than those of a normal distribution, as reported in [1,2]. Embrechts et al. [3] proposed the assumption that normal distribution will underestimate the risk associated with extreme tails. Since the 1990s, the extreme value theory (EVT) has been widely used in insurance, earthquake analysis, hydrology, transportation, climate, reliability analysis and other fields. The EVT mainly uses two approaches for modeling random variables: the block maxima model (BMM) and peaks over threshold (POT). The BMM first divides the sample interval, takes the maximum value in each sample interval, and then asymptotically fits the obtained maximum value series as the analysis object to the generalized extreme value (GEV) distributions. However, the POT fits all exceedances over a given threshold for heavy-tailed data. Pickands [4] first proposed that the excesses can be approximated via the generalized Pareto distribution (GPD) when the distribution of excesses is in the maximum domain of attraction. In the field of financial market analysis, risk measurement is an extremely important issue. As one of the most important and widely accepted risk measurement tools, Value at Risk (VaR) can reflect the risk and play an early-warning role in financial markets.

The VaR from the fitted GPD is extremely sensitive to the GPD parameter estimators and a small difference in the parameter value will cause a significant impact on a bank's financial position, highlighting the importance of accurately estimating GPD parameters.

Since Pickands first proposed the GPD, various parameter estimation methods for this distribution have been studied. For example, Hosking and Wallis [5] considered the method of moments (MOMs); Greenwood et al. [6] discussed probability weighted moments (PWMs); Smith [7] introduced maximum likelihood (ML); and Moharram et al. [8] discussed the least square (LS) of the GPD. Hosking [9] developed an L-moment method based on the PWM linear combination; Ashkar and Ouarda [10] proposed the generalized method of moments (GMOM) based on the MOM method. Castillo and Hadi [11] used the elemental percentile method (EPM). Based on the EPM, From and Ratnasingam [12] proposed various efficient closed-form estimators for the GPD. Product of spacing (POS) and logarithmic Cramér–von Mises (LCVM) methods were proposed at the same time. Rasmussen [13] proposed generalized probability weighted moments (GPWMs) based on the PWM method, both of which broadened the scope for parameter estimation. In recent years, for the estimation of GPD parameters, Zhang [14] introduced the likelihood moment estimator (LME), which solves the iterative convergence problem in ML methods. The LME always has the advantages of high asymptotic efficiency and simple calculation. Zhang and Stephens [15] combined Bayesian methods to propose an estimation method based on likelihood functions, which has strong practicality. Song and Song [16] considered the use of nonlinear least squares (NLSs) estimation. It is based on the least squares estimation method to minimize the sum of squares of the deviation between the empirical distribution function (EDF) and the theoretical distribution function (GPD) of the excess data. Park and Kim [17] developed weighted nonlinear least squares (WNLS) based on NLS, further improving the estimation accuracy of high quantiles. Based on the GPWM method, the generalized probability weighted moment equation (GPWME) method was proposed by Chen et al. [18], confirming that the GPWM method is a special case of the GPWME method, and the estimation method has no restrictions on parameter values. Chen et al. [19] combined the minimum distance estimation and the M-estimation in a linear regression. Martín et al. [20] proposed informative priors baseline Metropolis–Hastings (IPBMH) to improve the accuracy of Bayesian parameter estimation.

Choosing the appropriate threshold is a prerequisite for accurately estimating GPD parameters. If the selected threshold is too high, the actual sample size becomes smaller, resulting in too little data on the fitted excess distribution function such that the variance of the parameter estimate may be high. In contrast, if the selected threshold is too low, it may cause a biased estimate and an increase in estimated deviation. Several threshold selection procedures are available in the literature. Langousis et al. [21] detailed many of these methods for the chosen threshold. One category of methods applies the goodness of fit of the GPD. Choulakian and Stephens [22] proposed a goodness-of-fit test for a two-parameter GPD, using the Cramér–von Mises (CvM) and Anderson–Darling (AD) tests to select the lowest threshold at a given confidence level. Combining the AD and CvM tests with the stop rule proposed by G'Sell et al. [23], Bader et al. [24] proposed an automatic threshold selection method. Yang et al. [25] performed threshold selection based on the relationship between eigenvalues and thresholds. Saadatmand-Tarzjan [26] proposed a global threshold selection method based on fuzzy expert systems. Curceac et al. [27] used an automated threshold determination method based on the stability of shape parameters and modified scale parameters. Based on the L-moment theory, an automatic L-moment ratio threshold selection method was proposed by Silva Lomba and Fraga Alves [28].

In this study, within the POT framework, a new GPD parameter estimation method is provided to estimate VaRs. The method is derived from the GPWME method. The proposed method, however, is suitable for POT by employing the exceedances over a sufficiently high threshold. Firstly, based on the GPWME, we select three suitable objective functions, the specific forms of which can be found in Section 3.2. Secondly, using the exceedance over a certain high threshold for a heavy-tailed dataset, based on moment estimation and

the nonlinear weighted least squares methods, the sum of squared differences between the sample and population moments of a function of the GPD random variables is minimized. Finally, we select appropriate weights to modify the objective function to obtain a more accurate parameter estimate. Then, we estimate the extreme VaR via the proposed method. To evaluate its performance, we apply it to different heavy-tailed distributions and a real dataset. We then compare it to various common parameter estimation methods. The results show that our method performs better than the compared methods to some extent, particularly for VaRs with extremely high confidence levels in some cases.

This paper is organized as follows: In Section 2, the relevant theories in GPD, POT and VaR are briefly introduced. In Section 3, under the POT framework, we present a new GPD parameter estimator by comparing it with the existing method. Section 4 introduces numerical simulations, and we show the performance of different existing methods for estimating tail extreme quantiles under different heavy-tailed common parameter distributions. In Section 5, a similar exercise is performed using a real dataset. In Section 6, we conclude this paper.

2. EVT for Extreme Tail Risk Measures

2.1. The GPD

Let X be a random variable (r.v.). The cumulative distribution function (cdf) of the GPD is defined as

$$G_{\mu,\xi,\sigma}(x) = \begin{cases} 1 - \left(1 + \xi \dfrac{x-\mu}{\sigma}\right)^{-\frac{1}{\xi}}, & \xi \neq 0, \\ 1 - \exp\left(-\dfrac{x-\mu}{\sigma}\right), & \xi = 0, \end{cases} \tag{1}$$

where $\xi(\xi \in \mathbb{R})$, $\mu(\mu \in \mathbb{R})$ and $\sigma(\sigma > 0)$ are the shape, location, and scale parameters, respectively, and $1/\xi$ is the tail index. When $\mu = 0$, the three-parameter GPD reduces to the two-parameter GPD (ξ, σ). When $\xi > 0$, the domain of x is (μ, ∞) and $G_{\mu,\xi,\sigma}(x)$ is heavy-tailed. When $\xi < 0$, $x \in (\mu, \mu - \sigma/\xi)$, it is short-tailed. When $\xi = 0$, the GPD is a medium-tailed exponential distribution (more details can be found in [16]).

The corresponding probability density function (pdf) is

$$g_{\mu,\xi,\sigma}(x) = \begin{cases} \dfrac{1}{\sigma}\left(1 + \xi \dfrac{x-\mu}{\sigma}\right)^{-\frac{1}{\xi}-1}, & \xi \neq 0, \\ \dfrac{1}{\sigma}\exp\left(-\dfrac{x-\mu}{\sigma}\right), & \xi = 0. \end{cases}$$

In order to show the flexibility and asymmetry of the GPD, we plot the pdfs of the GPD with various shape parameters $\xi(\mu = 0, \sigma = 1)$ in Figure 1.

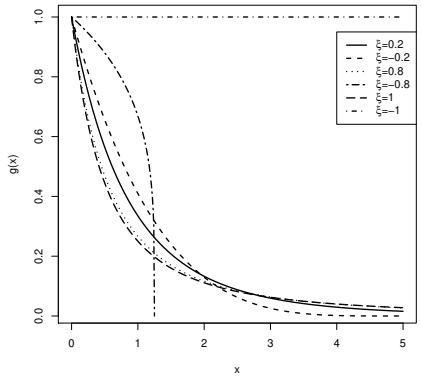

Figure 1. pdfs of GPD(μ, ξ, σ), $\mu = 0, \sigma = 1$.

The quantile function, $x(G)$, is

$$x(G) = \begin{cases} \mu - \frac{\sigma}{\xi}[1-(1-G)^{-\xi}], & \xi \neq 0, \\ \mu - \sigma \log(1-G), & \xi = 0. \end{cases}$$

2.2. Peaks over Threshold (POT)

The EVT mainly studies the tail distribution characteristics of the continuous r.v. X, that is, the tail of $F(x)$, $\bar{F}(x) = 1 - F(x)$, $0 < x < \infty$ and $\bar{F}(x)$ is also called the survival function [29]. If

$$\lim_{x\to\infty} \frac{\bar{F}(x\lambda)}{\bar{F}(x)} = \lambda^{-\alpha}, \lambda > 0,$$

we say that $\bar{F}$ changes regularly varying with index $\alpha > 0$ or $\bar{F} \in \Re_{-\alpha}$. When $\alpha = 0$, $\bar{F}$ is said to be slowly varying [17]. Based on this definition, there is a distribution that changes regularly as $\bar{F} \sim L(x)x^{-\alpha}$, where $L(\cdot)$ is slowly varying. It is known that $f(x) \sim g(x)$ means $\lim_{x\to\infty} \frac{f(x)}{g(x)} = 1$. It can be concluded that the tail of a regularly varying distribution can be expressed by multiplying a slowly varying function by a power function. At this point, the distribution is called the maximum domain of attraction of the Fréchet distribution ($F \in \mathrm{MDA}(\Phi_\alpha)$, where $\Phi_\alpha = \exp\{-x^{-\alpha}\}$), representing a distribution class with heavy tails if and only if $\bar{F} \in \Re_{-\alpha}$, where $\alpha > 0$. The GPD is in $\mathrm{MDA}(\Phi_\alpha)$ [17].

The Pickands–Balkema–de Haan theorem (see [4,29]) states that, for $\bar{F} \in \Re_{-\alpha}$, the excess loss $(X - u | X > u)$ from such a distribution with a high threshold $u > 0$ converges to the GPD with Pareto parameter $\xi > 0$ and $\frac{1}{\xi} = \alpha$. That is,

$$\lim_{u\to x_F} \sup_{0<x<x_F-u} |F_u(x) - G_{\xi,\sigma}(x)| = 0,$$

where $F_u(x) = P(X - u \leq x | X > u)$, and $x_F \leq \infty$ is the right endpoint of F. This means that the excess distribution $F_u(x)$ converges to the GPD when F is a heavy-tailed distribution in $\mathrm{MDA}(\Phi_\alpha)$ (see [4,29]).

It is worth noting that the GPD is stable with respect to excess over threshold operations [30]. This means that, if $X \sim \mathrm{GPD}(\xi, \sigma)$, the r.v. $Y = X - u | X > u$ will follow the GPD $(\xi, \sigma + \xi\mu)$, where u is a threshold. This can also be derived for any $\tilde{u} > u$, $X - \tilde{u} | X > \tilde{u}$ that follows a parameter of $(\xi, \sigma + \xi(u - \tilde{u}))$ of the GPD. This characteristic of the GPD illustrates that the excess above a threshold does not change the GPD shape parameter ξ, but the GPD scale parameter is altered.

2.3. Value at Risk (VaR)

VaR reflects the maximum possible loss of the value of a financial dataset or portfolio of securities within a future time period, under a given probability level. Let $F(x)$ be the distribution function of the population X; then, the p quantile of $F(x)$ is $F_X^{-1}(p)$, denoted by $Q_p(x) = F_X^{-1}(p)$. The exceedance distribution above the threshold u can be defined by [30]

$$F_u(x) = P(X - u \leq x | X > u) = \frac{F(u+x) - F(u)}{1 - F(u)}, 0 < x < x_F - u,$$

which is assumed to be $G_{\xi,\sigma}(x)$. Therefore, $F(x)$ can be expressed as

$$F(x) = (1 - F(u))G_{u,\xi,\sigma}(x) + F(u). \tag{2}$$

Based on the estimated parameters,

$$\hat{F}(x) = (1 - F_n(u))G_{u,\hat{\xi},\hat{\sigma}}(x) + F_n(u),$$

where F_n is the EDF, and $\hat{\xi}$ and $\hat{\sigma}$ are the estimations of the GPD parameters using the exceedances over the threshold. Then, the estimated p quantile of $F(x)$ is

$$\hat{Q}_p(X) = u + \frac{\hat{\sigma}}{\hat{\xi}}\left[\left(\frac{n}{n-n_u}(1-p)\right)^{-\hat{\xi}} - 1\right], \tag{3}$$

where n is the total sample size of observations, and n_u is the number of observations lower than the threshold u.

3. Parameter Estimation Method

3.1. Existing Method GPWME

Chen et al. [18] proposed the population GPWME, and defined $M_{g,r,s}(\theta)$ as follows

$$M_{g,r,s}(\theta) = E[g(Z;\theta)F_Z(Z;\theta)^r(1-F_Z(Z;\theta))^s], \tag{4}$$

where both r and s are real numbers, and $g(x)$ is a Borel measurable function for a parameter. Accordingly, the sample generalized probability weighted quasi-moment is defined as [18]

$$m_{g,r,s}(\theta) = \frac{1}{n}\sum_{i=1}^{n} g(Z_i;\theta)F_Z(Z_i;\theta)^r(1-F_Z(Z_i;\theta))^s. \tag{5}$$

For convenience, note that $X\sim$GPD(¸, œ) represents the excess threshold data, and the corresponding $F(x)$ represents the distribution function of the GPD. Denote $X_1, X_2, \ldots, X_n$ as a random sample of size n from $F(x)$ and denote $X_{1:n} < X_{2:n} < \cdots < X_{n:n}$ as order statistics. Chen et al. [18] set $\beta = -\xi/\sigma$, $g_1(x;\beta,\xi) = (1-\beta x)^{-\frac{1}{\xi}}$, $g_2(x;\beta,\xi) = \log(1-\beta x)$, $\beta < X_{n:n}^{-1}$. The population GPWMEs are

$$M_{g_1,0,s_1}(\beta,\xi) = E\left[(1-\beta X)^{-\frac{1}{\xi}}(1-F(X;\beta,\xi))^{s_1}\right] = \frac{1}{2+s_1}, \tag{6}$$

$$M_{g_2,0,s_2}(\beta,\xi) = -\xi E\{[\log(1-\beta X)](1-F(X;\beta,\xi))^{s_2}\} = \frac{\xi}{(1+s_2)^2}. \tag{7}$$

For the sample, when $s_1 > -2$, $s_2 > -1$,

$$m_{g_1,0,s_1}(\beta,\xi) = \frac{1}{n}\sum_{i=1}^{n}(1-\beta X_i)^{-1/\xi}(1-F(X_i;\beta,\xi))^{s_1}, \tag{8}$$

$$m_{g_2,0,s_2}(\beta,\xi) = \frac{1}{n}\sum_{i=1}^{n}[\log(1-\beta X_i)](1-F(X_i;\beta,\xi))^{s_2}. \tag{9}$$

Notice that

$$\frac{1}{n}\sum_{i=1}^{n} g_j(X_i;\beta,\xi)(1-F(X_i;\beta,\xi))^{s_j} = \frac{1}{n}\sum_{i=1}^{n} g_j(X_{i:n};\beta,\xi)(1-F(X_{i:n};\beta,\xi))^{s_j}, j = 1,2. \tag{10}$$

By combining Equations (6)–(10), we have

$$\frac{1}{n}\sum_{i=1}^{n}(1-\beta X_{i:n})^{-1/\xi}(1-p_{i:n})^{s_1} - \frac{1}{2+s_1} = 0, \tag{11}$$

$$\frac{1}{n}\sum_{i=1}^{n}(1-p_{i:n})^{s_2}\log(1-\beta X_{i:n}) - \frac{\xi}{(1+s_2)^2} = 0, \tag{12}$$

where $p_{i:n} = (i+\gamma)/(n+\delta)$ is the estimator of $F(X_{i:n};\beta,\xi)$, where $\delta = 0$ and $\gamma = 0.35$ [31]. The estimated values of β and ξ can be obtained from Equations (11) and (12), denoted by $\hat{\beta}_n$ and $\hat{\xi}_n$, from which $\hat{\sigma}_n = -\hat{\xi}_n/\hat{\beta}_n$ can be obtained.

3.2. New Methods

3.2.1. GWNLSM Estimation

GPWME applies parameter estimation where the $F(x)$ distribution is ideal. That is, in practice, for all observations, the specific distribution $F(x)$ is unknown in advance. It is known that, based on the Pickands–Balkema–de Haan theorem, the tail region of the observations can be modeled via the GPD. Therefore, a parameter estimate of the GPD is required. We propose an improvement on the method by combining it with the WNLS proposed by Park and Kim [17]. Therefore, generalized weighted nonlinear least squares moment (GWNLSM) estimation is proposed within the POT framework.

For the threshold u, data less than the threshold are recorded as 0, and for data greater than the threshold, the exceedance is defined as $X - u$. In order to obtain more accurate parameter estimates, the combination of the nonlinear least squares method and moment estimation is considered based on the GPWME method. The specific method is as follows.

Set

$$g_1(x;\xi,\sigma) = \left[1 + \frac{\xi}{\sigma}(x-u)\right]^{-1/\xi},$$

$$g_2(x;\xi,\sigma) = \log\left(1 + \frac{\xi}{\sigma}(x-u)\right),$$

$$g_3(x;\xi,\sigma) = 1.$$

Within the POT framework, $F(x)$ is replaced by Equation (2), and $F(u)$ is replaced by $F_n(u)$. Using Equations (4) and (5), we have

$$\begin{aligned} M_{g_1,0,s_1}(\xi,\sigma) &= E\left[\left(1 + \frac{\xi}{\sigma}(X_{i:n}-u)\right)^{-1/\xi}(1 - F(X_{i:n};\xi,\sigma))^{s_1}\right] \\ &= \frac{B(n+1, n+s_1+2-i)}{B(n-i+1, n+s_1+2)(1-F_n(u))}, \end{aligned}$$

$$\begin{aligned} M_{g_2,0,s_2}(\xi,\sigma) &= E\left\{\left[\log(1 + \frac{\xi}{\sigma}(X_{i:n}-u))\right](1 - F(X_{i:n};\xi,\sigma))^{s_2}\right\} \\ &= -\xi\frac{B(n+1, n+s_2+1-i)}{B(n-i+1, n+s_2+1)}\left(\sum_{j=n+s_2+1}^{n+s_2+i} j^{-1} + \log(1-F_n(u))\right), \end{aligned}$$

$$M_{g_3,0,1}(\xi,\sigma) = 1 - E[F(X_{i:n};\xi,\sigma)] = 1 - \frac{i}{n+1},$$

where $\xi > -\sigma/(X_{n:n}-u)$, $s_1 > -2$, $s_2 > -1$. The specific calculation process is shown in the Appendix A. For the sample moments, we have

$$\begin{aligned} m_{g_1,0,s_1}(\xi,\sigma) &= \left[1 + \frac{\xi}{\sigma}(X_{i:n}-u)\right]^{-1/\xi}[1 - F(X_{i:n};\xi,\sigma)]^{s_1} \\ &= [1-F_n(u)]^{s_1}\left(1 + \xi\frac{X_{i:n}-u}{\sigma}\right)^{(s_1+1)/\xi}, \end{aligned}$$

$$\begin{aligned} m_{g_2,0,s_2}(\xi,\sigma) &= \left[\log(1 + \frac{\xi}{\sigma}(X_{i:n}-u))\right](1 - F(X_{i:n};\xi,\sigma))^{s_2} \\ &= -\xi[1-F_n(u)]^{s_2}\left(1 + \xi\frac{X_{i:n}-u}{\sigma}\right)^{-s_2/\xi}\log\left(1 + \xi\frac{X_{i:n}-u}{\sigma}\right), \end{aligned}$$

$$m_{g_3,0,1}(\xi,\sigma) = 1 - F(X_{i:n};\xi,\sigma) = [1-F_n(u)](1-G(X_{i:n}-u)).$$

In the first step, the interim estimator $(\hat{\xi}_1, \hat{\sigma}_1)$ can be obtained via nonlinear minimization:

$$(\hat{\xi}_1, \hat{\sigma}_1) = \arg\min_{(\xi,\sigma)} \sum_{i=n_u+1}^{n} [M_{g_1,0,s_1}(\xi,\sigma) - m_{g_1,0,s_1}(\xi,\sigma)]^2, \tag{13}$$

The following second step with $(\hat{\xi}_1, \hat{\sigma}_1)$ as initial values and the third step with $(\hat{\xi}_2, \hat{\sigma}_2)$ as initial values lead to another optimization:

$$(\hat{\xi}_2, \hat{\sigma}_2) = \arg\min_{(\xi,\sigma)} \sum_{i=n_u+1}^{n} [M_{g_2,0,s_2}(\xi,\sigma) - m_{g_2,0,s_2}(\xi,\sigma)]^2, \tag{14}$$

$$(\hat{\xi}_3, \hat{\sigma}_3) = \arg\min_{(\xi,\sigma)} \sum_{i=n_u+1}^{n} [M_{g_3,0,1}(\xi,\sigma) - m_{g_3,0,1}(\xi,\sigma)]^2. \tag{15}$$

Based on the idea of weighted least squares regression, we find that the performance of the third step estimation $(\hat{\xi}_3, \hat{\sigma}_3)$ can be further improved by adding suitable weights in Equation (15). Set the weight to w_i=(Var$[F(X_{i:n})]$)$^{-2}$, where Var$[F(X_{i:n})] = \dfrac{i(n-i+1)}{(n+1)^2(n+2)}$. A revised version of the given nonlinear optimization is produced by adding weights:

$$(\hat{\xi}_3, \hat{\sigma}_3) = \arg\min_{(\xi,\sigma)} \sum_{i=n_u+1}^{n} w_i [M_{g_3,0,1}(\xi,\sigma) - m_{g_3,0,1}(\xi,\sigma)]^2. \tag{16}$$

Note that $M_{g_3,0,1}(\xi,\sigma) = 1 - \dfrac{i}{n+1}$; we modify $M_{g_3,0,1}(\xi,\sigma)$ as $1 - \dfrac{i-0.35}{n}$ to smooth the error of VaR via numerous simulations. Combined with Equations (13), (14) and (16), the GWNLSM was proposed. One advantage of the proposed GWNLSM over the GPWME is that it obtains a more stable extreme quantile estimator. The effect of the error is reduced because each squared deviation term is multiplied by the corresponding weight. The standard "optim" function in R is used to implement the GWNLSM estimator in our numerical studies.Without a loss of generality, we take all starting values as $(\xi, \sigma) = (0.1, 0.1)$ in the following simulation and application. When $\xi > 0$, the GPD is heavy-tailed. The proposed estimated method is only applicable to the statistical inference of the heavy-tailed GPD.

3.2.2. (s_1, s_2) Estimation

Based on the GWNLSM method, the values of s_1 and s_2 are calculated via a large number of simulations. With s_1 and s_2 fixed within a selection of ranges $(-2, 2)$ and $(0, 2)$, and a step size of 0.05, s_1 and s_2 have a total of 3280 pairs of combinations. A total of 3280 synthetic samples were employed to evaluate the root-mean-square error (RMSE) for VaR$_p$ of the fixed ξ, p, and $F_n(u)$ values. The values of ξ range from 0.1 to 0.9, the values of p are 0.999 and 0.9999 and those of $F_n(u)$ are 0.98, 0.99 and 0.995, where $p > F_n(u)$.

First, for a given ξ, p and $F_n(u)$, count the minimum and maximum values of the RMSE for VaR$_p$ corresponding to each set of parameters and then change the values of u and p, in turn, to calculate the corresponding RMSE values. Taking $\xi = 0.1$ as an example, because the values of u and p are different, there are seven combinations, based on the different values of s_1 and s_2, a total of seven sets of RMSEs are calculated. Specifically, when $F_n(u)$ is 0.98, p takes 0.99, 0.999, and 0.9999; when $F_n(u)$ is 0.99, p takes 0.999 and 0.9999; and when $F_n(u)$ is 0.995, p takes 0.999 and 0.9999. The results are shown in Table 1.

Table 1 shows the different values of ξ, p, and $F_n(u)$, as well as the corresponding actual number of samples used. The values in the table are estimated via the corresponding s_1 and s_2 values; then, the corresponding RMSE values are obtained, where min and max represent the minimum and maximum values of RMSE, respectively.

Table 1. s_1 and s_2 correspond to the RMSE values of VaR_p, where s_1 and s_2 are used in (13) and (14).

ξ	p = 0.99		p = 0.999		p = 0.9999	
	Min	**Max**	**Min**	**Max**	**Min**	**Max**
$n - n_u = 200$ ($F_n(u) = 0.98$)						
0.1	0.1505	0.1507	0.5241	0.5245	1.8920	1.8943
0.2	0.2417	0.3880	1.0468	1.9865	4.5350	5.9320
0.3	0.3874	0.5727	2.0901	3.3288	10.931	12.778
0.4	0.6203	0.6342	4.1739	4.2635	26.574	26.820
0.5	0.9916	1.0179	8.3218	8.4833	64.592	65.264
0.6	1.5879	1.6469	16.629	17.084	160.04	161.07
0.7	2.5359	2.6193	33.193	33.911	386.40	398.62
0.8	4.0551	4.2626	66.226	68.616	987.72	1012.01
0.9	6.4608	6.8859	132.31	136.16	2489.05	2655.14
$n - n_u = 200$ ($F_n(u) = 0.99$)						
0.1			0.5206	0.5465	2.0061	2.0466
0.2			1.0371	2.7049	4.8787	8.0178
0.3			2.0664	4.3109	11.912	16.020
0.4			4.1189	4.3153	29.4287	29.761
0.5			8.2235	8.6656	73.150	74.088
0.6			16.419	16.982	182.86	185.17
0.7			32.708	34.350	461.78	476.22
0.8			65.731	74.542	1184.33	1604.15
0.9			131.40	173.90	2853.84	3542.59
$n - n_u = 200$ ($F_n(u) = 0.995$)						
0.1			0.5544	0.6366	2.0507	2.2331
0.2			1.1021	2.5829	5.0543	8.8306
0.3			2.1912	4.2018	12.534	17.377
0.4			4.3598	4.5966	31.228	31.827
0.5			8.6729	9.1764	78.282	81.745
0.6			17.156	19.610	198.75	216.080
0.7			34.499	48.666	508.52	548.680
0.8			68.833	125.12	1301.21	1548.14
0.9			137.790	293.19	3388.58	5448.34

Second, for the given ξ and p, fix $F_n(u)$ as a certain value, and sort the RMSE values from smallest to largest, selecting the top 5% values and their corresponding s_1 and s_2. For these s_1 and s_2, they are weighted and averaged, with the weight being the reciprocal of the corresponding RMSE divided by the reciprocal sum of the RMSE. Taking $\xi = 0.1$ as an example, first sort the RMSE calculated by $F_n(u) = 0.98$ and $p = 0.99$ and select the first 5% of the lower RMSE values and their corresponding s_1 and s_2. Based on the selected RMSE value, the weighted averages of s_1 and s_2 are carried out to obtain the final weighted s_1 and s_2 values. The weights of s_1 and s_2 are the reciprocal of their corresponding RMSE divided by the reciprocal of the previous 5% RMSE. At this point, the s_1 and s_2 values corresponding to $\xi = 0.1$, and the $F_n(u) = 0.98$ and $p = 0.99$ can be calculated. Following the above steps, the s_1 and s_2 values corresponding to $F_n(u) = 0.98$, $p = 0.999$ and $p = 0.9999$ can also be calculated. This is the result based on $F_n(u)$ classification when $\xi = 0.1$. Similarly, we can obtain the result by fixing p as a certain value. By repeating the above steps, we can find the optimal values for s_1 and s_2.

Third, the values of s_1 and s_2 based on fixing $F_n(u)$ significantly fluctuate through calculation and comparison. Thus, the results of s_1 and s_2 based on fixing p are considered. Figure 2 is plotted in accordance with the p score, in which the upper three solid lines represent the image of s_1, the lower three dashed lines represent the image of s_2, and the different colored lines represent different values of p corresponding to VaR_p. From the image, it can be observed that the value of s_2 fluctuates very little and the basic value of s_2 is around 1, while the basic value of s_1 is negative and the change fluctuation is relatively

large. Based on the above analysis, $s_2 = 1$ and s_1 are used to find the function relationship. According to the results of s_1 and ξ, p shown in Figure 2, we can establish a linear regression model for s_1 via the "lm" function in R. Through a regression analysis of the value s_1 and ξ, p, the following model is obtained:

$$s_1 = 0.4\xi + 30p - 30. \tag{17}$$

Equation (17) first requires using the existing method to estimate ξ, and then determining s_2 according to the different p and ξ values; it is relatively troublesome to determine s_1. Therefore, RMSE is sorted from small to large. We select the first 30% of the data and their corresponding s_1 and value ranges, for a given p and $F_n(u)$; and then selects ξ to take the intersection of the value range of s_1 when taking different values, as the recommended value of s_1, that is, $s_1 = -1.15$. In the following simulation and application, the presented GWNLSM uses $s_1 = -1.15$ and $s_2 = 1$ for estimation parameters.

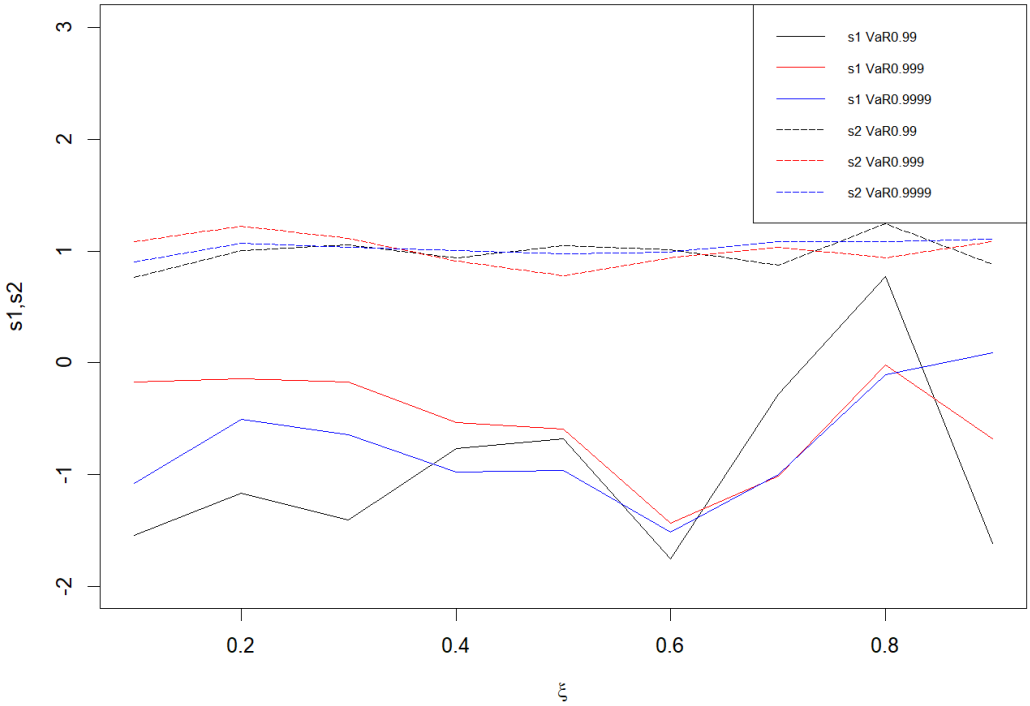

Figure 2. Plot of s_1 and s_2 with different ξ values (solid and dashed lines represent values of s_1 and s_2, respectively, while $p = 0.99, 0.999, 0.9999$).

4. Simulation Studies

We only choose heavy-tailed distributions since our main interest is heavy-tailed data. The performance of the proposed methods is investigated via Monte Carlo simulations. The competing estimators in clude the LME estimator by Zhang [14], the WNLS by Park and Kim [17], the GPWME by Chen et al. [18], and our GWNLSM method. In addition, besides the GPD simulated samples, we also generate samples from the Cauchy and Pareto distribution. The purpose is to evaluate the robustness of the proposed method when the population distribution is misjudged. Our focus is on estimating VaR rather than the GPD parameter itself; thus, the parameter estimation results are not shown. The 98th, 99th, and 99.5th sample quantiles are selected as the thresholds u for each sample, and the estimated extreme quantiles are VaR at 99%, 99.9%, and 99.99%, respectively. We summarize the simulation procedure as follows:

(1) Generate a sample from the given distribution, where the sample size is 10,000.
(2) Given $0 \ll F_n(u) < p < 1$, then $u = x_{F_n(u)}$.
(3) Estimate the parameters (ξ, σ) and the VaR (given in Equation (3)).

(4) Repeat steps (1)–(3) 2000 times.
(5) Compute the RMSE and the absolute relative bias (ARB) of each VaR estimator.

Note that there are 50–200 observations with different thresholds for the GPD fit, with a total sample size of 10,000.

It can be seen that there is a reasonable number of exceedances for researching extreme tails. Tables 2 and 3 show the simulation results. Table 2 is based on the simulation data generated via the GPD, using different estimation methods to estimate VaR and calculate the corresponding index values. Table 3 uses the simulation data generated from the Cauchy distribution and Pareto distribution to estimate VaR. To highlight the objective under the condition of satisfying heavy-tailed distribution characteristics, our method proves to be effective even when the specific distribution form is incorrectly determined.

Example 1. *GPD(ξ, σ) with different ξ values and $\sigma = 1$.*

As can be seen from Table 2, by comparison, the LME and WNLS perform better for estimating VaR at 99% in terms of RMSE and ARB. However, with an increasing p in the estimated quantile, the proposed GWNLSM's performance improves. Overall, the GWNLSM is relatively stable. In all cases of estimation for VaR at 99.99%, the GWNLSM outperforms all other estimators in terms of the RMSE, regardless of the used threshold value. Notably, it can be seen that when ξ is relatively small, the LME estimate is relatively accurate. As ξ increases, the GWNLSM estimation error decreases, resulting in more accurate estimates compared to the other methods in most cases, as assessed via RMSE and ARB. In addition, as the threshold increases, the GWNLSM exhibits a smaller ARB for VaR at 99.99% compared to the other methods.

In order to facilitate the comparison and illustrate the effect of method improvement, we use $F_n(u) = 0.995$, $p = 0.9999$, and $p = 0.999$ as examples to draw comparisons, as shown in Figures 3–8. The abscissa of Figures 3–8 is the value of ξ, where the ordinates in Figures 3, 4, 6 and 7 represent the RMSE of VaR and the ordinates in Figures 5 and 8 represent the ARB of VaR. We generate 10,000 samples from the GPD with $\sigma = 1$ and ξ ranging from 0.1 to 1. This process is repeated 2000 times to calculate the RMSE and ARB of VaR at 99.99% and 99.9%. In terms of the RMSE and ARB of VaR at 99.99% and 99.9%, to better illustrate the advantages of the different estimation methods and show a discernible difference among curves in Figures 3 and 6, we provide Figures 4 and 7 as exploded views of Figures 3 and 6, respectively. Here, in order to save space, we have only drawn a partial trend chart. In Figures 3–8, we can see that the GWNLSM method performs better overall. For the RMSE evaluation criteria, GWNLSM estimation performed well in most cases. In terms of the ARB evaluation criteria, when ξ is lower, the LME estimates VaR more accurately, and when ξ is larger, the GWNLSM estimates VaR more accurately.

Example 2. *Cauchy (μ, σ). The cdf of the Cauchy distribution is defined as*

$$F_{\mu,\sigma}(x) = \frac{1}{\pi} \arctan\left(\frac{x-\mu}{\sigma}\right), \quad -\infty < x < +\infty,$$

where μ and σ are location and scale parameters.

We generated samples from the standard Cauchy distribution ($\mu = 0$, $\sigma = 1$) and presented the results in Table 3 with different thresholds. Table 3 illustrates that the GWNLSM outperforms other methods at 99.9% and 99.99% in terms of the RMSE and ARB with the 99th and 99.5th sample quantiles as thresholds.

Table 2. RMSE and ARB are calculated for each VaR estimation from the GPD with different ξ values.

		RMSE			ARB		
		VaR 99%	**VaR 99.9%**	**VaR 99.99%**	**VaR 99%**	**VaR 99.9%**	**VaR 99.99%**
GPD (0.2, 1)							
$F_n(u) = 0.98$	LME	0.2358	1.0236	4.6917	0.0249	0.0548	0.1364
	WNLS	0.2363	1.1068	5.1240	0.0250	0.0600	0.1528
	GPWME	0.2406	1.0464	5.1278	0.0255	0.0558	0.1459
	GWNLSM	0.2423	1.0412	4.5217	0.0253	0.0564	0.1388
$F_n(u) = 0.99$	LME		1.0274	5.2043		0.0550	0.1511
	WNLS		1.0902	5.6780		0.0590	0.1715
	GPWME		1.0388	5.9179		0.0555	0.1661
	GWNLSM		1.0350	4.8295		0.0559	0.1484
$F_n(u) = 0.995$	LME		1.0889	5.4096		0.0581	0.1559
	WNLS		1.0973	5.6234		0.0592	0.1718
	GPWME		1.0928	6.0105		0.0582	0.1675
	GWNLSM		1.0959	5.0130		0.0589	0.1534
GPD (0.4, 1)							
$F_n(u) = 0.98$	LME	0.5960	4.1581	28.526	0.0359	0.0889	0.2208
	WNLS	0.5963	4.3481	29.282	0.0359	0.0945	0.2346
	GPWME	0.6043	4.2111	30.011	0.0364	0.0897	0.2286
	GWNLSM	0.6210	4.1443	26.543	0.0369	0.0905	0.2209
$F_n(u) = 0.99$	LME		4.1749	33.105		0.0893	0.2527
	WNLS		4.3218	33.957		0.0939	0.2705
	GPWME		4.2194	36.377		0.0901	0.2708
	GWNLSM		4.1020	29.095		0.0892	0.2411
$F_n(u) = 0.995$	LME		4.3559	35.972		0.0927	0.2684
	WNLS		4.3036	34.655		0.0935	0.2800
	GPWME		4.3624	38.747		0.0928	0.2800
	GWNLSM		4.3250	30.981		0.0932	0.2542
GPD (0.8, 1)							
$F_n(u) = 0.98$	LME	3.8021	68.581	1157.57	0.0624	0.1704	0.4027
	WNLS	3.7820	67.292	1054.26	0.0623	0.1720	0.3890
	GPWME	3.8128	68.095	1142.27	0.0627	0.1690	0.3976
	GWNLSM	4.0488	65.579	989.23	0.0656	0.1697	0.3828
$F_n(u) = 0.99$	LME		69.805	1480.19		0.1732	0.4870
	WNLS		68.472	1349.27		0.1753	0.4726
	GPWME		70.129	1520.94		0.1739	0.4998
	GWNLSM		65.032	1155.32		0.1674	0.4314
$F_n(u) = 0.995$	LME		71.113	1812.26		0.1758	0.5483
	WNLS		67.375	1436.30		0.1726	0.5027
	GPWME		71.083	1799.72		0.1758	0.4694
	GWNLSM		67.983	1292.96		0.1720	0.4694
GPD (2, 1)							
$F_n(u) = 0.98$	LME	981.834	3.28×10^{6}	1.32×10^{9}	0.1535	0.4490	1.1581
	WNLS	958.756	2.78×10^{5}	8.93×10^{7}	0.1511	0.4028	0.8835
	GPWME	961.981	3.11×10^{5}	1.11×10^{8}	0.1508	0.4311	1.0458
	GWNLSM	3257.37	4.49×10^{5}	5.82×10^{7}	0.5939	0.8414	0.9610
$F_n(u) = 0.99$	LME		3.58×10^{6}	2.65×10^{9}		0.4786	1.72649
	WNLS		3.02×10^{6}	1.56×10^{9}		0.4339	1.2574
	GPWME		3.57×10^{5}	2.29×10^{8}		0.4793	1.6624
	GWNLSM		4.89×10^{5}	5.23×10^{7}		0.9684	1.0007
$F_n(u) = 0.995$	LME		3.59×10^{5}	6.07×10^{8}		0.4777	2.5958
	WNLS		2.96×10^{5}	2.45×10^{8}		0.4268	1.5203
	GPWME		4.26×10^{5}	7.44×10^{8}		0.5410	4.5462
	GWNLSM		4.79×10^{5}	4.99×10^{7}		0.9568	0.9976

Example 3. *Pareto* (σ, μ, α).

The cdf of the Pareto (type I) distribution is given by

$$F(x) = 1 - \left(\frac{x-\mu}{\sigma}\right)^{-\alpha}, \quad x \geq \mu + \sigma,$$

where μ, σ, and α are the location, scale, and shape parameters.

The Pareto distribution is also another heavy-tailed distribution. We generated Pareto samples with $\sigma = 1$ and $\alpha = 1$, and the results are presented in Table 3. As can be seen in Table 3, in most cases, our proposed method performs best again.

Table 3. RMSE and ARB for different heavy-tailed distributions.

		RMSE			ARB		
		VaR 99%	**VaR 99.9%**	**VaR 99.99%**	**VaR 99%**	**VaR 99.9%**	**VaR 99.99%**
Cauchy (0, 1)							
$F_n(u) = 0.98$	LME	3.1092	88.443	2318.32	0.0775	0.2120	0.4773
	WNLS	3.0863	85.680	2033.446	0.0772	0.2121	0.4527
	GPWME	3.0866	87.650	2230.66	0.0770	0.2095	0.4681
	GWNLSM	3.3829	82.235	1949.25	0.0839	0.2078	0.4417
$F_n(u) = 0.99$	LME		90.650	3202.64		0.2166	0.5904
	WNLS		85.880	2707.33		0.2138	0.5293
	GPWME		90.269	3123.24		0.2158	0.5799
	GWNLSM		82.370	2462.95		0.2066	0.5153
$F_n(u) = 0.995$	LME		91.416	4325.15		0.2178	0.7113
	WNLS		84.334	3070.36		0.2111	0.5997
	GPWME		91.209	4022.12		0.2175	0.6959
	GWNLSM		85.447	3379.91		0.2106	0.5925
Pareto (1, 1)							
$F_n(u) = 0.98$	LME	9.3271	280.801	7496.16	0.0756	0.21743	0.5073
	WNLS	9.3032	270.150	6702.71	0.0754	0.21501	0.4791
	GPWME	9.3260	278.776	7322.52	0.0755	0.2163	0.5041
	GWNLSM	10.079	263.021	6286.66	0.0814	0.2126	0.4683
$F_n(u) = 0.99$	LME		286.769	9886.04		0.2208	0.6097
	WNLS		271.847	8537.50		0.2168	0.5585
	GPWME		286.754	9904.80		0.22084	0.6094
	GWNLSM		262.670	7461.39		0.2110	0.5345
$F_n(u) = 0.995$	LME		287.946	14914.1		0.2212	0.7202
	WNLS		265.757	10433.2		0.2133	0.6269
	GPWME		287.636	13634.9		0.2210	0.7170
	GWNLSM		274.081	9534.50		0.2161	0.6060

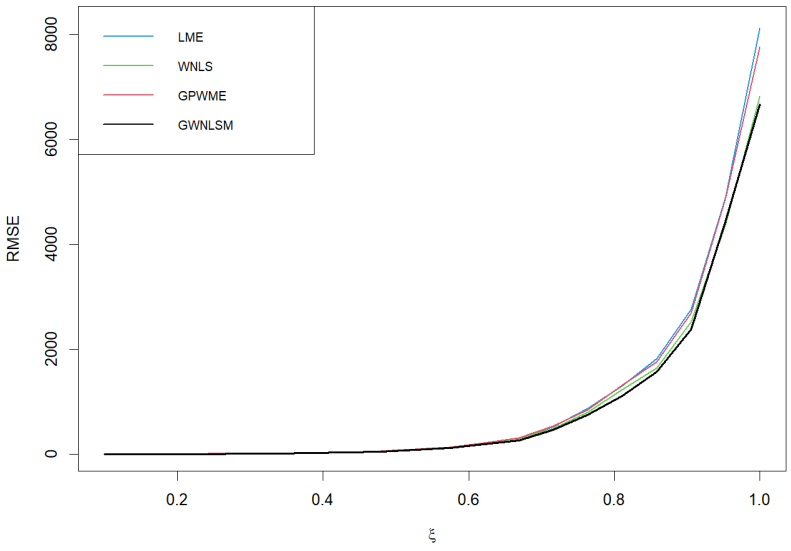

Figure 3. RMSE of VaR at 99.99% with $\sigma = 1$ and 98th quantile as threshold.

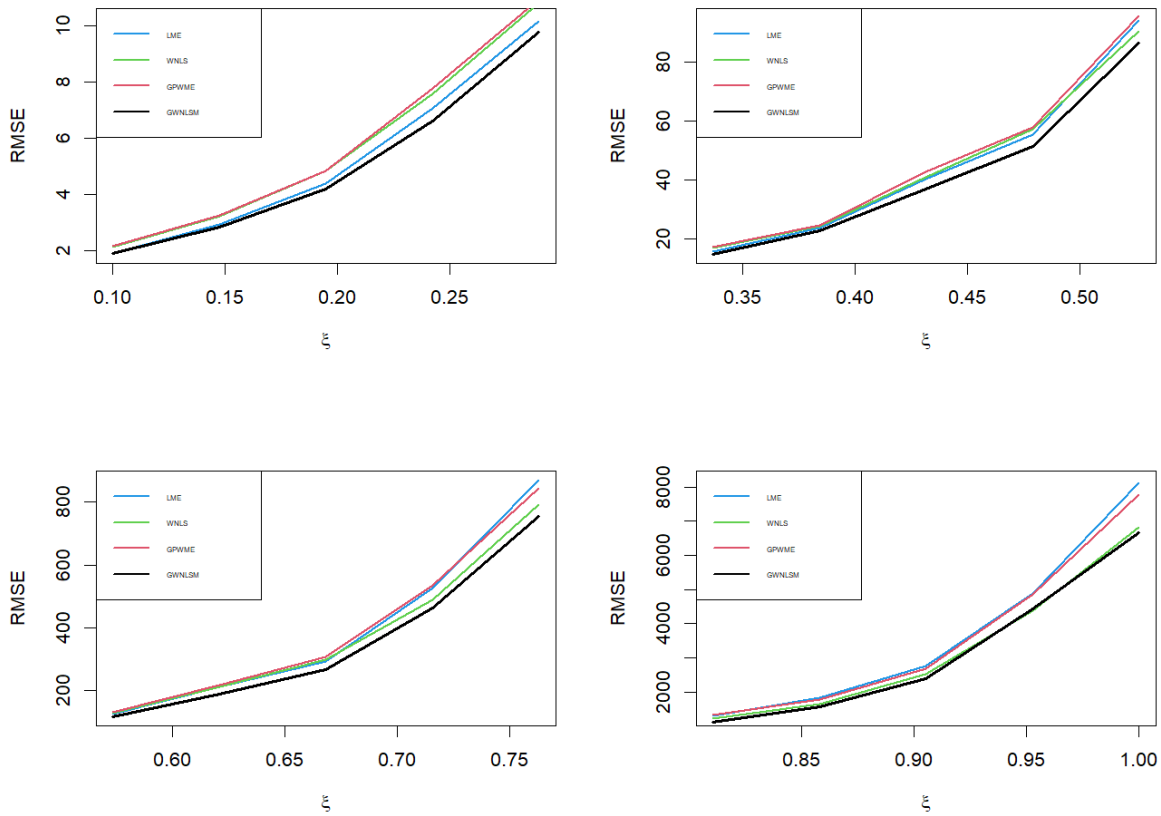

Figure 4. RMSE of VaR at 99.99% with $\sigma = 1$ and 98th quantile as threshold (exploded view of Figure 3).

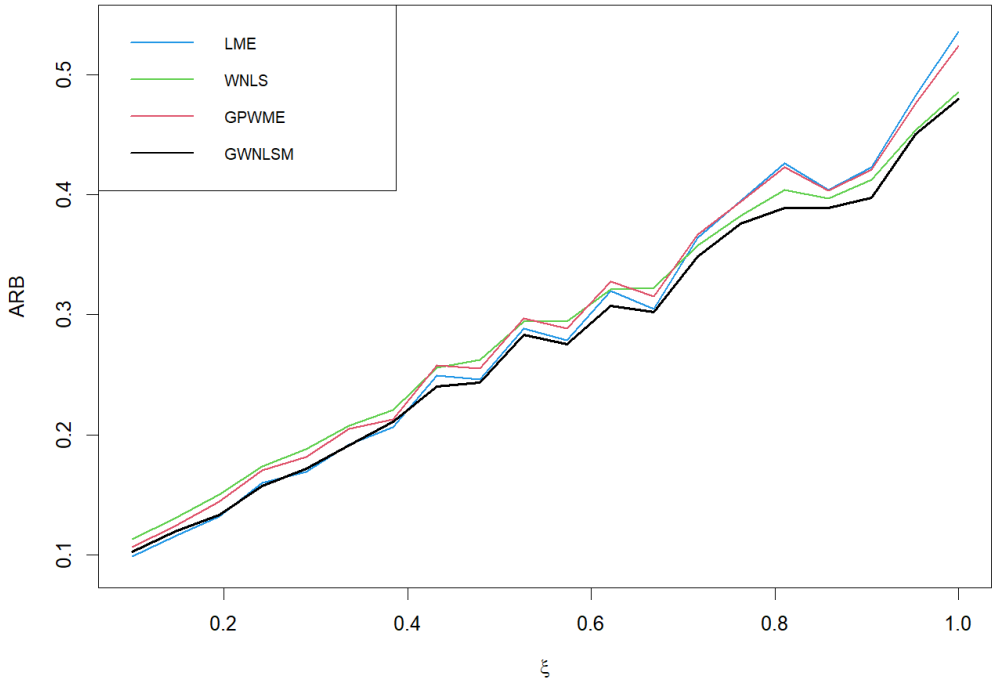

Figure 5. ARB of VaR at 99.99% with $\sigma = 1$ and 98th quantile as the threshold.

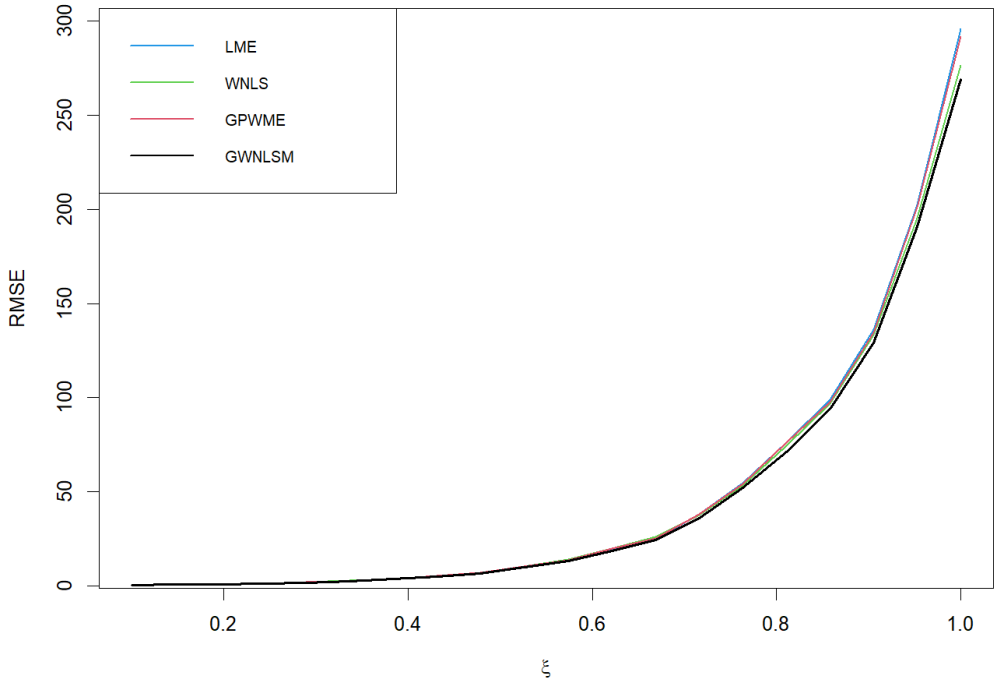

Figure 6. RMSE of VaR at 99.9% with $\sigma = 1$ and 98th quantile as threshold.

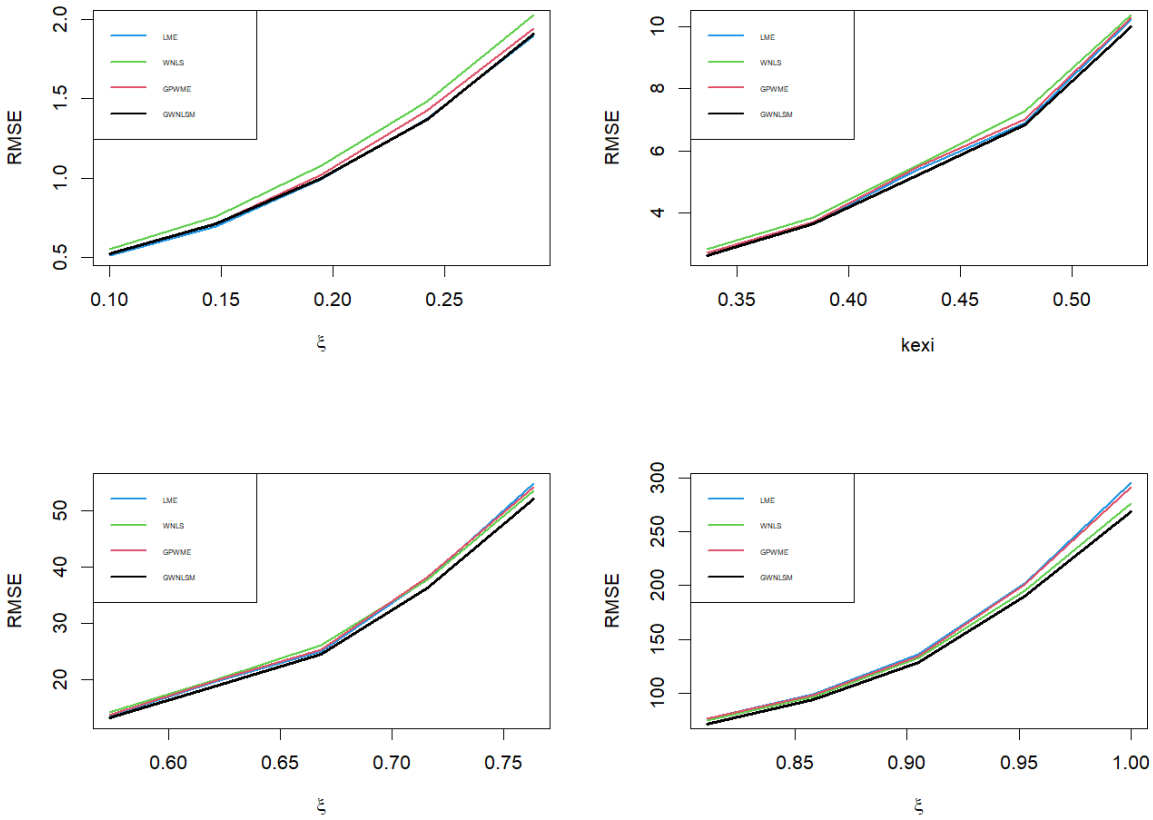

Figure 7. RMSE of VaR at 99.9% with $\sigma = 1$ and 98th quantile as the threshold (exploded view of Figure 6).

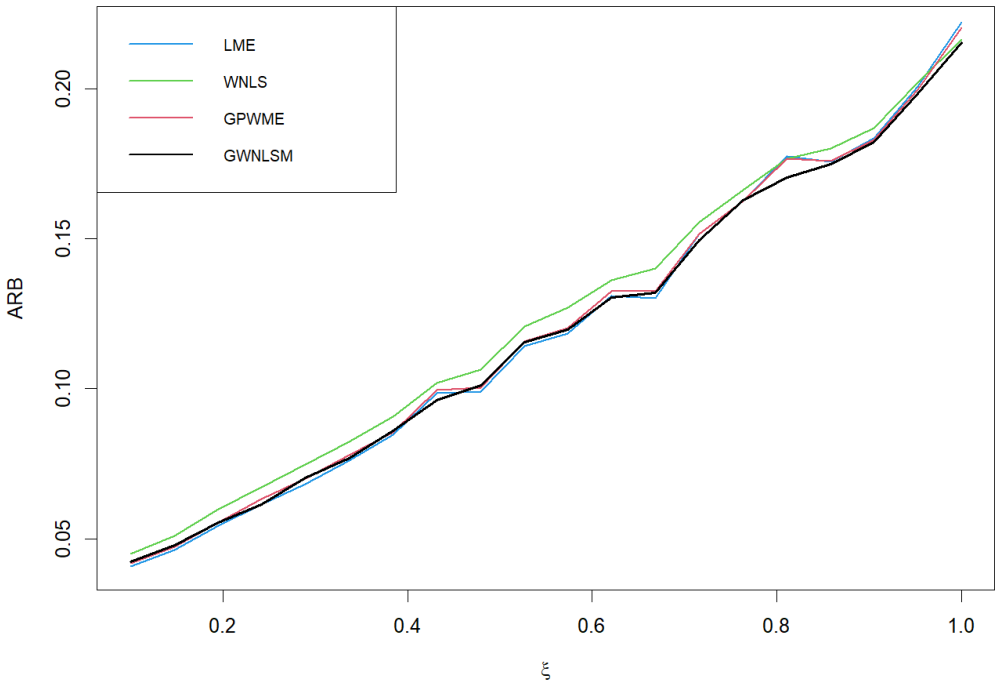

Figure 8. ARB of VaR at 99.9% with $\sigma = 1$ and 98th quantile as threshold.

As can be seen from Table 3, for the Cauchy and the Pareto distributions, the GWNLSM parameter estimation method performs relatively well, regardless of a high- or low-threshold u, and the accuracy requirements of the estimated VaR are evidently superior. The higher the accuracy of the estimate, the more obvious the contrast error of various methods appears, and it is evident that the GWNLSM methods exhibit superiority over the LME, WNLS and GPWME methods in terms of performance. Whether it is a Cauchy or Pareto distribution, GWNLSM is optimal in most cases for VaR at 99.9% and VaR at 99.99%.

5. Actual Data Processing and Analysis

To verify the performance of different estimators, we chose $PM_{2.5}$ data for our experimental analysis. $PM_{2.5}$ data were obtained from the China National Environmental Monitoring Center. The center is a national technical institution and is directly affiliated with the Ministry of Ecology and Environment. It operates as the center of technology, network, information, quality control, and training for national environmental monitoring. In addition, it collects at least 100 million environmental monitoring data annually, which provides a strong guarantee for scientifically and accurately assessing national environmental quality. The $PM_{2.5}$ monitoring results are also published online (https://www.cnemc.cn/ (accessed on 19 February 2023) We use the Beijing $PM_{2.5}$ dataset from 2015 to 2022. The sample size is 2737. In order to preserve the original nature of the data and reduce the influence of scale parameter σ of the GPD, making it as small as possible, we changed the data separately, with the $PM_{2.5}$ dataset reduced to 1% of the original. The following results are calculated based on transformed data.

We select the threshold and the corresponding analysis calculation using the following steps. First, when the exponential QQ plot is convex, indicating that the empirical quantile is growing faster than the theoretical quantile, the distribution is heavy-tailed. Conversely, the explanation is a short-tailed distribution. The tail distribution characteristics of $PM_{2.5}$ are examined. The exponential QQ plot is given in Figure 9. It is worth noting that, in the exponential QQ plot of this study, the x axes are theoretical quantiles, and the y axes are empirical quantiles. Contrary to the aforementioned theory QQ, Figure 9 shows a concave shape; it can be observed that the data used are subject to a heavy-tailed distribution.

For the heavy-tailed features of the diagnostic data, we also plotted the empirical mean excess function (EMEF), given in Figure 10. In general, if EMEF has a significant

linear change after exceeding a certain threshold and the slope is positive, it indicates that the excess threshold data follow the GPD and the shape parameter is greater than 0. For heavy-tailed data, this threshold can be selected as the threshold for analysis; if EMEF has a significant linear change after a certain threshold, but the slope is negative, it indicates that the observed data are short-tailed. As can be seen from Figure 10, the dataset satisfied the heavy-tailed distribution.

Secondly, a suitable threshold is selected. The preliminary value of the threshold can be roughly observed in the mean residual life plot. Another way to initially select a threshold is through the Hill plot in Figure 10. The trend stabilization point of the Hill plot is generally determined as a threshold. By observing the EMEF and Hill plots in Figure 10, it can be intuitively judged that the u value is about 1.

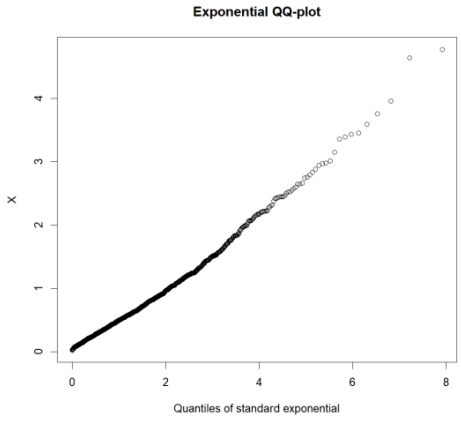

Figure 9. The QQ diagram of the $PM_{2.5}$ data; the ordinate x represents order data.

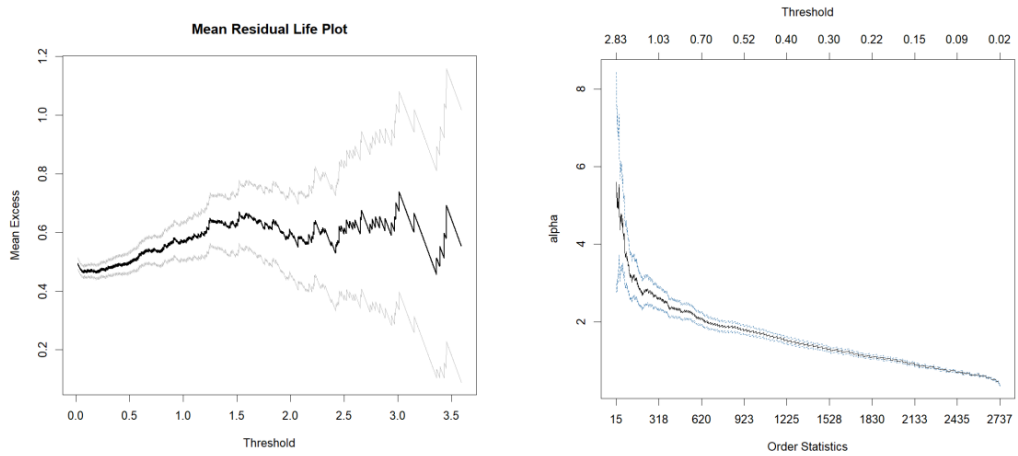

(a) The EMEF diagram (b) The Hill diagram

Figure 10. The EMEF and Hill diagrams of the $PM_{2.5}$ data. In (**a**), the black and grey lines represent the empirical mean residual life and its confidence intervals with confidence level 0.95. In (**b**), the black and blue lines represent the Hill estimator of the GPD tail index and its confidence intervals with confidence level 0.95.

In order to find a more suitable and objective threshold u, we use goodness-of-fit tests to select the threshold. The main objective is to find the lowest threshold such that the highest number of exceedances above the threshold follows the GPD. We use the AD test statistic [22].

The details of the threshold selection method, instance calculation, and simulation steps are as follows.

(1) Threshold selection. For the $PM_{2.5}$ data, we combine the AD statistic and the Raw Down method to select the threshold $u = 0.83$, exceeding the number $n - n_u = 473$,

$F_n(u) = 82.72\%$, where Raw Down means that the test begins at the largest threshold and choose the first threshold until the test is rejected, then the threshold before the rejection is chosen [24].

(2) Based on the threshold u using LME, WNLS, and GPWME, the GWNLSM method is used to calculate the estimates of $\hat{\xi}$, $\hat{\sigma}$ and $\mathrm{VaR_t}$ (given in Equation (3)). The specific results are shown in Table 4.

(3) Based on the above parameter estimation results, $n - n_u$ random samples following $\mathrm{GPD}(u, \hat{\xi}, \hat{\sigma})$ and $\tilde{\xi}$, $\tilde{\sigma}$, $\mathrm{VaR_s}$ are calculated.

(4) Repeat (3) 1000 times; RMSE and ARB for VaR are calculated. Some results are shown in Table 5.

Table 4. Parameter estimation for real data using different methods.

	$\hat{\xi}$	$\hat{\sigma}$
LME	0.0782	0.5185
WNLS	0.1169	0.4953
GPWME	0.0813	0.5169
GWNLSM	0.0481	0.5363
u	0.83	

Table 5 compares the index values of the VaR based on four parameter estimation methods for the $PM_{2.5}$ data. From Table 5, we can see that the LME and proposed GWNLSM exhibit better performances for VaR at 99.9% and VaR at 99.99% in terms of RMSE and ARB. Specifically, it can be observed that the proposed method works better for VaR at 99.99% in most cases.

Table 5. VaR estimation of the $PM_{2.5}$ data.

	RMSE			**ARB**		
	VaR at 99%	**VaR at 99.9%**	**VaR at 99.99%**	**VaR at 99%**	**VaR at 99.9%**	**VaR at 99.99%**
LME						
LME	0.939642	3.567475	9.359341	0.029951	0.069050	0.140593
WNLS	1.114730	4.347896	11.12457	0.049561	0.102806	0.165263
GPWME	1.033365	4.195512	11.23957	0.045660	0.096672	0.161397
GWNLSM	1.021122	3.781147	9.356901	0.045634	0.083634	0.140933
WNLS						
LME	1.068671	4.288407	11.87006	0.032968	0.077429	0.136665
WNLS	1.194244	4.963725	13.53752	0.037138	0.091490	0.159159
GPWME	1.110651	4.800949	13.69599	0.034303	0.086194	0.155536
GWNLSM	1.097004	4.361997	11.53057	0.034309	0.080041	0.136313
GPWME						
LME	0.729066	2.94535	8.193269	0.025959	0.061376	0.1145927
WNLS	0.787671	3.432898	9.433241	0.028197	0.072860	0.132312
GPWME	0.739436	3.287148	9.479313	0.026414	0.068239	0.128704
GWNLSM	0.745556	3.017241	8.055831	0.026776	0.064257	0.114585
GWNLSM						
LME	1.596907	4.875529	10.94257	0.041240	0.083499	0.134014
WNLS	1.889057	5.813446	12.88081	0.049464	0.101360	0.160320
GPWME	1.739965	5.616292	12.95679	0.045003	0.095299	0.155665
GWNLSM	1.651400	4.856433	10.34925	0.043370	0.083253	0.132417

6. Conclusions

In this study, based on the GPWME method within the POT framework, we present a novel GPD parameter estimation GWNLSM. The proposed method is applicable to the heavy-tailed GPD when the shape parameter ξ is greater than 0. This method utilizes the concepts of nonlinear least squares estimation and moment estimation while applying

GPWME to the POT framework. In terms of the RMSE and ARB, extensive simulation studies and real-world datasets have shown that the advantage of the newly proposed estimator when VaRs are at high confidence levels. For example, when the estimated extreme quantile VaR is 99.99%, GWNLSM is optimal in most cases. Furthermore, when a set of data satisfies other heavy-tailed distributions, we can still use the asymmetrical GPD to obtain approximate extreme quantile estimates. The resulting extreme quantile estimates also exhibit relatively small errors. The new method performs well for heavy-tailed Cauchy and Pareto distributions and the actual dataset we present. A future research direction involves exploring more accurate and simpler methods to estimate the GPD parameters within the POT framework and optimizing the selection of s_1 and s_2.

Author Contributions: Formal analysis, W.C. (Wenru Chen) and X.Z.; funding acquisition, X.Z., H.C., Q.J. and W.C. (Weihu Cheng); supervision, X.Z., H.C. and W.C. (Weihu Cheng); validation, X.Z., H.C. and W.C. (Weihu Cheng); writing—original draft, W.C. (Wenru Chen), X.Z., M.Z. and Q.J.; writing—review and editing, W.C. (Wenru Chen) and X.Z. All authors have read and agreed to the published version of the manuscript.

Funding: The authors would like to thank the National Office for Philosophy and Social Sciences (grant number: 20BTJ054) for their support.

Data Availability Statement: The data are published in https://www.cnemc.cn/ (accessed on 19 February 2023).

Acknowledgments: The authors would like to thank the referees and editors for their very helpful and constructive comments, which have significantly improved the quality of this paper.

Conflicts of Interest: The authors declare no conflicts of interest.

Appendix A

This section gives the calculation process of $M_{g_i,0,s_i}(\xi,\sigma), i = 1,2,3$ in detail.

Suppose that we have a sample $X_1, X_2, \ldots, X_n$ of size n. For convenience, we write $F(X_{i:n})$ as F_i, where F_i follows Beta$(i, n-i+1)$. Hence, we have

$$\begin{aligned} E[-\log(1-F_i)] &= \frac{\Gamma(n+1)}{\Gamma(i)\Gamma(n+1-i)} \int_0^1 -x^{i-1}(1-x)^{n-i}\log(1-x)\mathrm{d}x \\ &= \sum_{j=1}^{i} \frac{1}{n+1-j}. \end{aligned}$$

and

$$\begin{aligned} E(1-F_i)^a &= \frac{\Gamma(n+1)}{\Gamma(i)\Gamma(n+1-i)} \int_0^1 x^{i-1}(1-x)^{n+a-i}\mathrm{d}x \\ &= \frac{\Gamma(n+1)\Gamma(n+a+1-i)}{\Gamma(n+1-i)\Gamma(n+a+1)} \\ &\triangleq h(a). \end{aligned}$$

Hence,

$$\begin{aligned} M_{g_1,0,s_1}(\xi,\sigma) &= \frac{1}{1-F(u)} E(1-F_i)^{s_1+1} \\ &= \frac{\Gamma(n+1)\Gamma(n+s_1+2-i)}{\Gamma(n-i+1)\Gamma(n+s_1+2)(1-F(u))}. \end{aligned}$$

At the same time, we can also obtain the following results

$$E[(1-F_i)^{s_2}(-\log(1-F_i))] = \frac{\Gamma(n+1)}{\Gamma(i)\Gamma(n+1-i)}\int_0^1 -x^{i-1}(1-x)^{n+s_2-i}\log(1-x)\mathrm{d}x$$
$$= h(s_2)\sum_{j=1}^{i}\frac{1}{n+s_2+1-j}.$$

Therefore,

$$M_{g_2,0,s_2}(\xi,\sigma) = -\xi\log(1-F(u))E(1-F_i)^{s_2} - \xi E[(1-F_i)^{s_2}(-\log(1-F_i))]$$
$$= -\xi\log(1-F(u))h(s_2) - \xi h(s_2)\sum_{j=1}^{i}\frac{1}{n+s_2+1-j}$$
$$= -\xi h(s_2)\left[\log(1-F(u)) + \sum_{j=1}^{i}\frac{1}{n+s_2+1-j}\right],$$

and

$$M_{g_3,0,1}(\xi,\sigma) = E(1-F_i) = h(1) = 1 - \frac{i}{n+1}.$$

References

1. Tawn, J.A. Bivariate extreme value theory: Models and estimation. *Biometrika* **1988**, *75*, 397–415. [CrossRef]
2. Tawn, J.A. Modelling multivariate extreme value distributions. *Biometrika* **1988**, *77*, 245–253. [CrossRef]
3. Embrechts, P.; Resnick, S.I.; Gennady, S. Extreme Value Theory as a Risk Management Tool. *N. Am. Actuar. J.* **1999**, *3*, 30–41. [CrossRef]
4. Pickands, J. Statistical inference using extreme order statistics. *Ann. Stat.* **1975**, *3*, 119–131.
5. Hosking, J.R.; Wallis, J.R. Parameter and quantile estimation for the generalized pareto distribution. *Technometrics* **1987**, *29*, 339–349. [CrossRef]
6. Greenwood, J.A.; Landwehr, J.M.; Matalas, N.C.; Wallis, J.R. Probability weighted moments: Definition and relation to parameters of several distributions expressable in inverse form. *Water Resour. Res.* **1979**, *15*, 1049–1054. [CrossRef]
7. Smith, R.L. Maximum likelihood estimation in a class of nonregular cases. *Biometrika* **1985**, *72*, 67–90. [CrossRef]
8. Moharram, S.; Gosain, A.; Kapoor, P. A comparative study for the estimators of the generalized pareto distribution. *J. Hydrol.* **1993**, *150*, 169–185. [CrossRef]
9. Hosking, J.R. L-moments: Analysis and estimation of distributions using linear combinations of order statistics. *J. R. Stat. Soc. Ser. B (Methodol.)* **1990**, *52*, 105–124. [CrossRef]
10. Ashkar, F.; Ouarda, T.B. On some methods of fitting the generalized pareto distributions. *J. Hydrol.* **1996**, *177*, 117–141. [CrossRef]
11. Castillo, E.; Hadi, A.S. Fitting the generalized pareto distribution to data. *J. Am. Stat. Assoc.* **1997**, *92*, 1609–1620. [CrossRef]
12. From, S.G.; Ratnasingam, S. Some efficient closed-form estimators of the parameters of the generalized pareto distribution. *Environ. Ecol. Stat.* **2022**, *29*, 827–847. [CrossRef]
13. Rasmussen, P.F. Generalized probability weighted moments: Application to the generalized pareto distribution. *Water Resour. Res.* **2001**, *37*, 1745–1751. [CrossRef]
14. Zhang, J. Likelihood moment estimation for the generalized pareto distribution. *Aust. N. Z. J. Stat.* **2007**, *49*, 69–77. [CrossRef]
15. Zhang, J.; Stephens, M.A. A new and efficient estimation method for the generalized pareto distribution. *Technometrics* **2009**, *51*, 316–325. [CrossRef]
16. Song, J.; Song, S. A quantile estimation for massive data with generalized pareto distribution. *Comput. Stat. Data Anal.* **2012**, *56*, 143–150. [CrossRef]
17. Park, M.H.; Kim, J.H. Estimating extreme tail risk measures with generalized pareto distribution. *Comput. Stat. Data Anal.* **2016**, *98*, 91–104. [CrossRef]
18. Chen, H.; Cheng, W.; Zhao, J.; Zhao, X. Parameter estimation for generalized Pareto distribution by generalized probability weighted moment-equations. *Commun.-Stat.-Simul. Comput.* **2017**, *46*, 7761–7776. [CrossRef]
19. Chen, P.; Ye, Z.S.; Zhao, X. Minimum distance estimation for the generalized pareto distribution. *Technometrics* **2017**, *59*, 528–541. [CrossRef]
20. Martín, J.; Parra, M.I.; Pizarro, M.M.; Sanjuán, E.L. Baseline methods for the parameter estimation of the generalized pareto distribution. *Entropy* **2022**, *24*, 178. [CrossRef] [PubMed]
21. Langousis, A.; Mamalakis, A.; Puliga, M.; Deidda, R. Threshold detection for the generalized pareto distribution: Review of representative methods and application to the noaa ncdc daily rainfall database. *Water Resour. Res.* **2016**, *52*, 2659–2681. [CrossRef]

22. Choulakian, V.; Stephens, M.A. Goodness-of-fit tests for the generalized pareto distribution. *Technometricsh* **2001**, *43*, 478–484. [CrossRef]
23. G'Sell, M.G.; Wager, S.; Chouldechova, A. Sequential selection procedures and false discovery rate control. *J. R. Stat. Ser. B Stat. Methodol.* **2016**, *78*, 423–444. [CrossRef]
24. Bader, B.; Yan, J.; Zhang, X. Automated threshold selection for extreme value analysis via ordered goodness-of-fit tests with adjustment for false discovery rate. *Ann. Appl. Stat.* **2018**, *12*, 310–329. [CrossRef]
25. Yang, X.; Zhang, J.; Ren, W.X. Threshold selection for extreme value estimation of vehicle load effect on bridges. *Int. J. Distrib. Sens. Netw.* **2018**, *14*, 1–12. [CrossRef]
26. Annabestani, M.; Saadatmand-Tarzjan, M. A new threshold selection method based on fuzzy expert systems for separating text from the background of document images. *Iran. J. Sci. Technol. Trans. Electrical Eng.* **2019**, *43*, 219–231. [CrossRef]
27. Curceac, S.; Atkinson, P.M.; Milne, A.; Wu, L.; Harris, P. An evaluation of automated GPD threshold selection methods for hydrological extremes across different scales. *J. Hydrol.* **2020**, *585*, 124845. [CrossRef]
28. Silva Lomba, J.; Fraga Alves, M.I. L-moments for automatic threshold selection in extreme value analysis. *Stoch. Environ. Res. Risk Assess.* **2020**, *34*, 465–491. [CrossRef]
29. Balkema, A.A.; De Haan, L.I. Residual life time at great age. *Ann. Probab.* **1974**, *2*, 792–804. [CrossRef]
30. De Zea Bermudez, P.; Kotz, S. Parameter estimation of the generalized Pareto distribution—Part I. *J. Stat. Plan. Inference* **2010**, *140*, 1353–1373. [CrossRef]
31. Landwehr, J.M.; Matalas, N.; Wallis, J. Estimation of parameters and quantiles of wakeby distributions. *Water Resour. Res.* **1979**, *15*, 1361–1372. [CrossRef]